ANL-7752

Argonne National Laboratory

MELTDOWN ANALYSIS OF VARIOUS EBR-II CORE CONFIGURATIONS USING THE MELT-II CODE

by

G. H. Golden and R. H. Shum

Printed in the United States of America
Available from
National Technical Information Service
U.S. Department of Commerce
Springfield, Virginia 22151
Price: Printed Copy $3.00; Microfiche $0.65

ANL-7752
Reactor Technology

ARGONNE NATIONAL LABORATORY
9700 South Cass Avenue
Argonne, Illinois 60439

MELTDOWN ANALYSIS OF VARIOUS EBR-II CORE CONFIGURATIONS USING THE MELT-II CODE

by

G. H. Golden and R. H. Shum

EBR-II Project

November 1970

TABLE OF CONTENTS

LIST OF FIGURES

LIST OF TABLES

MELTDOWN ANALYSIS OF VARIOUS EBR-II CORE CONFIGURATIONS USING THE MELT-II CODE

by

G. H. Golden and R. H. Shum

ABSTRACT

Effects of unbounded input-reactivity ramps on three types of EBR-II core configurations were studied with the MELT-II code. One core contained only metal fuel and was similar to the wet-critical configuration; a second was a hypothetical mixed-oxide configuration; and a third contained both fuels in amounts typical of a recent irradiation configuration of the reactor. Feedback reactivity was assumed to be due to axial expansion of fuel, and, after melting, to gravity-induced fuel collapse. Collapse was taken to begin at a given point in the reactor when one of four specified input temperatures was exceeded; these temperatures were related to the fuel and cladding melting points or eutectic temperature and the normal boiling point of the coolant.

The resulting model for noncoherent collapse resulted in much smaller collapse reactivity rates than those predicted earlier by use of a model for simple, coherent collapse. Also, the metal-fuel core would approach a disassembly condition only for input-reactivity ramps of about 20 dollars/sec or greater; the oxide-fuel core would approach disassembly for input ramps as low as 1 dollar/sec; and the mixed-fuel core would behave like the metal-fuel core. The results indicate that the EBR-II core should always have some metal fuel to protect it from rapid disassembly.

I. INTRODUCTION

The primary containment system of the EBR-II reactor was designed to contain a release of nuclear energy that was estimated from a modified Bethe-Tait analysis, the rate of reactivity input being determined by coherent slumping of the core under gravity.[1,2] More recent analyses have modified the original conclusions.

The specific slumping model for the original analysis assumed that the sodium coolant had boiled out of the middle of the core and the uranium

in this region had trickled down into the bottom of the core, to form a region of high uranium density with a void above it. This initial fuel movement from a region of high worth to one of lower worth would decrease k_{eff} by about 0.1. At this point, the upper portion of the core was assumed to begin falling freely toward the dense lower portion. Parametric studies showed that the calculated maximum rate of reactivity insertion at the point of prompt criticality (600 dollars/sec) occurred when 10% of the middle region melted and was redistributed in the lower 45% of the core, and the upper 45% began its free fall. If the control rods were initially withdrawn, the reactor would be further subcritical when the upper portion began to fall; this condition would lead to maximum rates of reactivity insertion of up to 800-1000 dollars/sec. A Bethe-Tait analysis for a reactivity insertion of 1000 dollars/sec at prompt criticality gave a nuclear-energy yield of 2.4×10^9 J, of which about 80% was assumed to be converted to mechanical energy.

Current methods of analysis show that the above result is unrealistically conservative. (This conservatism was recognized by the designers of EBR-II, who based the primary containment upon release of mechanical energy of only about a third of that originally calculated.)

The original result is unrealistic for two reasons. First, the conversion of nuclear to mechanical energy is much less efficient than 80%, typically being about 1-10%.[3] Second, more realistic models for gravity-induced core collapse, which relate local collapse to time-dependent local temperatures, give much smaller reactivity rates than those resulting from coherent collapse for the three-zone model.

A study has been made to demonstrate the smaller reactivity rates. A model (which assumes collapse) contained in the MELT-II computer code was used.[4] Three types of EBR-II cores were considered:

(1) An all-metal-fuel core very similar to the wet-critical configuration of EBR-II;

(2) A hypothetical oxide-fuel core; and

(3) A core, containing both metal and oxide fuel, that was very similar to a recent irradiation configuration of the reactor (run 37).

For each of these core types, the production of fuel collapse by various unbounded input-reactivity ramps, and the subsequent interactions of reactivity effects, were investigated.

II. MELT-II CALCULATIONS

A. Description and Application of MELT-II Code

The MELT-II code[4] predicts the neutronic and thermal-hydraulic effects of power and flow transients on a sodium-cooled fast reactor. The code couples the six-delayed-group point-kinetics equations with a detailed multichannel time-dependent heat-transfer scheme, and it treats reactivity feedback due to fuel expansion, Doppler effect, sodium voiding, and fuel collapse. Also, a delayed scram trip can be initiated for specified values of overpower, period, and coolant outlet temperature.

In this work, some features of the code were not used. The Doppler effect was neglected because Tdk/dT was found to be only -0.0003 for a hypothetical all-oxide-fuel configuration of EBR-II.[5] The effect would be the largest for the oxide configuration. Sodium voiding was not included because: (a) the sodium-void effect in EBR-II is negative (hence not accounting for it should in general lead to overestimating the rise in core temperature and energy release); and (b) the specific model used for voiding had not been checked. As worst cases, input ramps of reactivity were assumed to be unbounded; i.e., the scram-trip option of the code was not used. Thus, the net reactivity as a function of time was determined only by the input-reactivity ramp and the feedback due to fuel expansion and collapse.

In the MELT-II code, one fuel element and its associated coolant are used to represent the average behavior of a row of subassemblies in the reactor, and the time-dependent heat transfer is calculated for every axial node of each such element. In each such node, temperatures are monitored at:

(1) The fuel centerline;

(2) A specified radial node in the fuel, e.g., near its surface;

(3) The cladding (midwall); and

(4) The coolant.

Whenever any one of the above temperatures exceeds a specified value, cladding failure is assumed, with the fuel in that node and every node above beginning to fall according to the equation

$$\frac{d^2H}{dt^2} + \xi \frac{dH}{dt} = -g,$$

where H is the position at time t, ξ is a damping factor, and g is the acceleration due to gravity. Here ξ was taken equal to zero; i.e., fuel slumping was determined only by gravity. (The specification of temperatures leading to cladding failure is discussed in Sect. II.B.5.)

In each time increment, the net change in reactivity due to fuel slumping is found by summing over all spatial nodes the change in fuel mass in each node multiplied by the fuel worth in that node. The fuel worth in each node is input as a table. Thus the major assumptions in this slumping model are that melting fuel falls out of the bottom of the core (i.e., it does not accumulate at the core bottom), and that the spatial variation of the fuel worth is not distorted by the slumping fuel (i.e., the extent of slumping is small during the transient).

The reactivity due to fuel expansion is now calculated in MELT-II by multiplying the average core temperature coefficient of reactivity due to axial expansion of the fuel by the change in the average core-fuel temperature. This approximation causes the fuel-expansion reactivity to be underestimated for the core center and overestimated for the outer rows.

The present studies arbitrarily assume disassembly of the core to be imminent if the peak fuel temperature corresponds to the boiling point of the fuel at 1 atm. The code is written so that a given problem can readily be run beyond this point to generate a range of input conditions for a disassembly code such as VENUS.[6]

B. Input for Calculations

Required input for MELT-II includes data on core geometry, neutronics, thermal-hydraulics, fuel properties, power conditions, and reactivity. The input ramp is entered as a table of reactivity versus time. With a special option of the code, the kinetics subroutine is bypassed and power is calculated directly by interpolation of a table of power normalized to the steady-state value versus time. This option was used in the synthesis technique for treating cores containing more than one type of fuel.

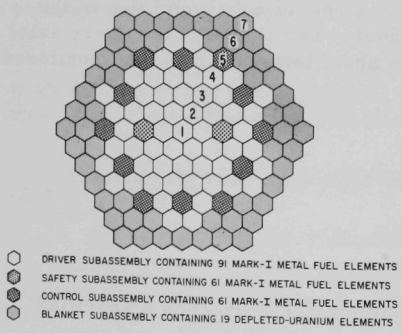

Fig. 1. Core Loading: All Metal Fuel

1. Core Geometries

Figure 1 shows the loading for the all-metal-fuel core, which is similar to the EBR-II wet-critical configuration.[7] The Mark-I metal fuel element consists of a 5% fissium-95% uranium (48.1% enriched) alloy pin, 0.144-in. in diameter x 14.22 in. long, in a 0.174-in.-OD, 0.009-in.-wall, Type 304 stainless-steel tube.[1] The annulus between the pin and the tube is filled with sodium as a thermal bond, and 0.049-in.-dia Type 304 stainless-steel spacer wire is wrapped helically around the tube. A driver

subassembly contains 91 metal fuel elements, and a control or safety subassembly contains 61 metal elements. In rows 8-16 are blanket subassemblies containing depleted uranium.

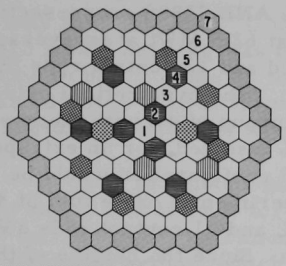

Fig. 2. Core Loading: Oxide Fuel

The loading for the hypothetical oxide core is shown in Fig. 2. The fuel element is a 0.220-in.-OD, 0.016-in.-wall, Type 316 stainless-steel tube containing 14.22 in. of helium-bonded U-20 wt % PuO_2 fuel of 85% smeared density and has a 0.051-in. spacer wire. A subassembly contains 61 mixed-oxide elements, and safety and control subassemblies each contain 37 oxide elements. The core also contains nine experimental subassemblies containing oxide fuel (here assumed identical to the driver subassemblies) plus four experimental structural subassemblies containing 50 vol % Type 316 stainless steel and 50 vol % sodium. In rows 7-11 are subassemblies containing nickel reflector elements, and in rows 12-16 are subassemblies containing depleted-uranium blanket elements.

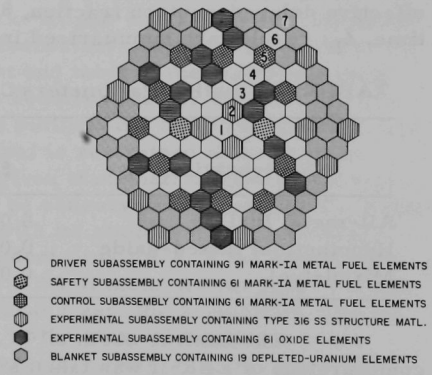

Fig. 3. Core Loading: Mixed Fuel

The loading to represent EBR-II as an irradiation facility (see Fig. 3) was taken from a thermal-hydraulics study made on various EBR-II configurations;[8] it is similar to the run-37 configuration. The metal fuel element is the Mark IA, which differs from the Mark I in having a somewhat shorter fuel height (13.5 versus 14.22 in.) and a somewhat higher uranium enrichment (51.9 versus 48.1%). A driver subassembly contains 91 Mark-IA elements, and a safety or control subassembly contains 61 of them. The mixed-oxide fuel element differs from that used in the hypothetical oxide core in being shorter (13.5 versus 14.22 in.) and having highly enriched uranium (92.7 versus 54.8%). An experimental oxide subassembly has 61 mixed-oxide elements. The experimental structural subassemblies are 50 vol % Type 316 stainless steel and 50 vol % sodium.

2. Neutronics

Neutronics calculations were made with the MACH-1 one-dimensional diffusion-theory package[9] and the ANL 23806 cross-section set. The all-metal-fuel reactor would be critical at 62.5 MWt at an average burnup of 1% with the two safety rods fully inserted and 12 control rods 85% inserted, for an extrapolated height of 64.54 cm. The hypothetical oxide core would be critical at 62.5 MWt at an average burnup of 4% with the two safety rods fully inserted and eight control rods 85% inserted, for an extrapolated height of 64.38 cm. Similarly, the mixed-fuel configuration would be critical at 62.5 MWt with the metal fuel at 1% and experimental oxide fuel at 4% average burnup, the two safety rods fully inserted, and 11 control rods 85% inserted, for an extrapolated height of 64.40 cm. Since the heights of the all-metal-fuel and hypothetical oxide-fuel cores were both 14.22 in., however, it was desirable to make comparative MELT-II calculations on a mixed-fuel configuration having the same height and nearly the same axial power shape. For all three configurations, steady-state power distributions were estimated from reaction rates by isotope and region, as described in Ref. 8. The power distribution for the all-metal-fuel configuration was also used in the thermal-hydraulics code SNAFU[8] to check the steady-state temperature distribution predicted by MELT-II; agreement was good.

The BAILIFF subroutine in MACH 1 was used to estimate the effective delayed-neutron fraction, β_{eff}, and the prompt-neutron generation time, ℓ_p; results are summarized in Table I.

TABLE I. Kinetics Parameters Calculated from BAILIFF Subroutine

Configuration	β_{eff}	ℓ_p, sec	$\frac{Ih}{1\%\ \Delta k/k}$
All-metal fuel	0.00717	0.793×10^{-7}	434
Hypothetical mixed-oxide	0.00578	2.204×10^{-7}	516
Mixed-fuel	0.00692	0.862×10^{-7}	445

The central worth of 93.2% enriched uranium in the wet-critical configuration of EBR-II was taken as 257 Ih/kg.[10] From this value, the central worth of the Mark-I fuel containing 95% uranium, 48.1% enriched, was estimated as

$$257 \frac{Ih}{kg} \times \frac{0.481}{0.932} \times 0.95 \times \frac{0.01\ \Delta k/k}{434\ Ih} = 2.903 \times 10^{-3} \frac{\Delta k/k}{kg}.$$

The spatial distribution of fuel worth for this configuration was determined in studies made on a ZPR-III critical assembly.[11] The central worth of the oxide fuel was estimated similarly, with an assumed fuel composition of

20 wt % PuO_2 (80 wt % ^{239}Pu, 20 wt % ^{240}Pu);

80 wt % UO_2 (54.84 wt % ^{235}U, 45.16 wt % ^{238}U).

With only the ^{239}Pu and ^{235}U in the oxide fuel accounted for, a central worth of 3.413×10^{-3} $\Delta k/k$-kg was obtained; the spatial distribution of worth was assumed to be the same as that for the wet-critical configuration. Because the mixed-oxide core is larger than the wet-critical one, the estimated distribution of oxide-fuel worth is too high.

For the mixed-fuel configuration, separate problems were run for the metal driver fuel, for safety and control subassemblies containing metal fuel, and for experimental subassemblies containing oxide fuel. For a driver-fuel problem, which involved the first six rows of the reactor, each value in the original worth table for metal fuel was multiplied by 0.97528 (i.e., 434/445). The safety and control subassemblies were in the third and fifth rows, respectively; here the row-3 and -5 results from the foregoing modification were used. The oxide experiments were in rows 3-6; the fuel worths for these rows were taken as those for the corresponding rows in the hypothetical oxide configuration multiplied by 1.1596 (i.e., 516/445).

The core-average linear temperature coefficient of reactivity for the all-metal-fuel core was taken as that of the Mark-I fuel in the wet-critical configuration,[1] -3.9×10^{-6} $\Delta k/k$-°K, and was assumed independent of the state of the fuel. Because this coefficient accounted for most of the negative feedback during each transient and most of the fuel would melt during each transient, this assumption requires further discussion. The volumetric expansion coefficient of the molten fuel should be greater than that of the solid. Thus, if the molten fuel is restrained so as to move mostly in the axial direction during a given transient, the use of the temperature coefficient of the solid would be conservative. Because the uranium fuel forms a low-melting eutectic with its stainless-steel cladding, however, there is a temperature-dependent time limit on the restraining ability of the cladding--about 1 sec for EBR-II metal driver fuel.[12] Thus, for transients occurring in less than about 1 sec, the assumption that the temperature coefficient is independent of the state of the fuel appears justifiable. It becomes increasingly suspect, however, with longer and longer transients. On the other hand, other temperature coefficients that were neglected (e.g., those due to expansion of coolant and structure, which have a similar effect) become increasingly important for longer transients. (The coolant-density coefficient is -8.7×10^{-6} $\Delta k/k$-°K.[1]) A quantitative understanding of this complex problem would require an appropriate experimental program.

The corresponding temperature coefficient for the hypothetical oxide core is difficult to estimate, even for the solid fuel, because of possible

mechanical interaction between fuel and cladding and the sensitivity of the interaction to operating history. Thus, in this work two different temperature coefficients for the oxide were arbitrarily assumed; one was equal to, and another was one-third of, that for the metal-fuel core.

The MELT-II calculations for the all-metal-fuel and hypothetical oxide-fuel cores were based upon the total driver subassemblies in each core; i.e., they did not specifically consider the reactivity feedback effects of safety, control, and fuel-bearing experimental subassemblies. Most of the feedback effect was due to fuel expansion, and hence was approximated by using the full core-average fuel-expansion coefficients for only the driver subassemblies. In the analysis of the mixed-fuel configuration, specific account was taken of the other types of subassemblies present.

The temperature coefficient of the set of safety and control subassemblies in the mixed-fuel configuration was estimated as

$$(\Delta k/k\text{-}^\circ K)_{s+c} = -3.9 \times 10^{-6}\left(\frac{n_s}{n_t} \cdot \frac{W_3}{\overline{W}} + \frac{n_c}{n_t} \cdot \frac{W_5}{\overline{W}}\right)\frac{434}{445},$$

where, for the all-metal-fuel core,

n_s = number of safety elements in core = 2 x 61 = 122,

n_c = number of control elements in core = 11 x 61 x 0.85 = 570,

n_t = total number of safety, control, and driver elements in core = 5879,

W_3 = axially averaged worth of fuel in row 3 = 2.029×10^{-3} $\Delta k/k$-kg,

W_5 = axially averaged worth of fuel in row 5 = 1.092×10^{-3} $\Delta k/k$-kg,

and

$\overline{W}$ = core-average fuel worth = 1.080×10^{-3} $\Delta k/k$-kg.

Thus, $(\Delta k/k\text{-}^\circ K)_{s+c} = -5.21 \times 10^{-7}$. Similarly, for the experimental oxide fuel having one-third the temperature coefficient of the metal fuel, $(\Delta k/k\text{-}^\circ K)_{ox} = -2.68 \times 10^{-7}$; and for the driver fuel in the first and second iteration problems, $(\Delta k/k\text{-}^\circ K)_{D,1} = -3.80 \times 10^{-6}$ and $(\Delta k/k\text{-}^\circ K)_{D,2} = -3.12 \times 10^{-6}$.

3. Thermal-Hydraulics

For consistency with EBR-II hazards calculations reported earlier,[1] most of the cases studied here corresponded to a power near that of the source (8 W) and 5.5% of full flow (only the auxiliary EM pump operating). For the all-metal-fuel reactor, the full coolant flow per subassembly for each type and position was taken from Ref. 1. For the

hypothetical oxide core, full flow corresponded to orificing to produce an average core ΔT of 190°F in each row at a total reactor power of 62.5 MWt. The full flow rates in the driver, safety, and control subassemblies in the mixed-fuel core were taken from Ref. 1. The flow rates in the experimental oxide subassemblies in rows 3-6 of this core were determined by the average ΔT of 190°F used for the hypothetical oxide core, but differed from the corresponding flow rates for the oxide core, owing to the somewhat different radial power distributions.

A gap conductance of 0.567 J/sec-cm^2-°K (1000 Btu/hr-ft^2-°F) was assumed for the helium-bonded oxide fuel element. The heat-transfer coefficient of sodium for the 5.5%-flow cases was approximated as

$$h = k/\Delta r,$$

where k is the thermal conductivity of sodium at an assumed average temperature[13] of 800°F, and Δr is the difference between the average outer radius of the flow channel and the outer radius of the associated element. Thus, for the metal and oxide elements, h = 10.06 and 9.23 J/sec-cm^2-°K, respectively. For full flow, h was taken as 13.28 J/sec-cm^2-°K (24,300 Btu/hr-ft^2-°F).

4. Fuel Properties

The fuel[1] for the all-metal core is an alloy of uranium containing 5% fission-product metals and having a room-temperature density of 17.95 g/cm^3. The heat content above 0°C for this alloy is shown in Fig. 4.[14] Because MELT-II as written does not treat solid-state phase transformations, the curve in the temperature range of interest was approximated by the heavy straight lines in the figure. Thus, for the U-5 Fs alloy, the specific heat was assumed constant at 0.282 J/g-°C below the pseudomelting point of 1010°C, and constant at 0.136 J/g-°C above this temperature. The heat of fusion was taken as 69.4 J/g. The normal boiling point was that estimated for pure uranium, 4146°C.[15] The change in thermal conductivity of U-5 Fs with temperature was tabulated input.[16]

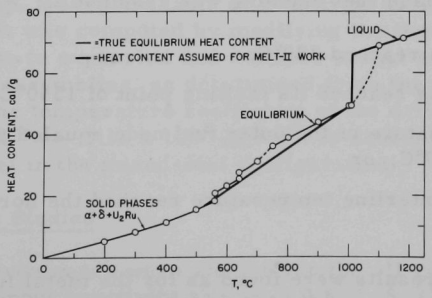

Fig. 4
Heat Content above 0°C of Uranium-5% Fissium

The corresponding properties for the mixed-oxide fuel were:[17]

Density	9.85 g/cm^3
Solid specific heat	$(0.3884 - 1.619 \times 10^{-4}T + 8.781 \times 10^{-8}T^2)$ J/g-°K
Liquid specific heat	0.548 J/g-°K
Melting point	2767°C
Heat of fusion	280 J/g
Normal boiling point	3677°C

The thermal conductivity as a function of temperature was tabulated input.

5. Temperatures Causing Cladding Failure

Cladding failure was assumed to occur when any one of a set of four temperatures identified with a given axial node in a given row exceeded a specified value. For the metal fuel, failure was assumed if:

a. The sodium coolant reached its normal boiling point of 880°C, with consequent vapor blanketing;

b. The cladding reached the fuel pseudomelting point of 1010°C,

c. The temperature in the outer radial fuel node was 10°C above the fuel pseudomelting point; or

d. The fuel centerline temperature reached the arbitrarily set high value of 1827°C.

With these criteria, initial cladding failure would result from criterion a for input reactivity ramps of 1 dollar/sec or less, and from criterion c for ramps of 5 dollars/sec or greater.

Failure of the oxide fuel cladding was assumed if:

a. The sodium reached 880°C;

b. The cladding reached its melting point of 1350°C;

c. The temperature of the outer fuel node equaled the fuel melting temperature of 2767°C; or

d. The fuel centerline temperature reached the normal boiling point of 3677°C.

Here the same results were found as for the metal fuel.

C. Treatment of Two-fuel Cores

Differences between results of MELT-II calculations on the all-metal-fuel and all-oxide-fuel core configurations (see Sect. III) suggested a corresponding analysis of an irradiation configuration of EBR-II containing both types of fuel. Because the code now can treat only one fuel, an iterative approach was necessary to approximate the reactivity feedback due to each type of fuel at a given point in time. This approach is as follows for the example of a 5-dollar/sec unbounded ramp input of reactivity to the mixed-fuel reactor initially at 5.5% of full flow and 8 W of power:

1. A MELT-II problem was run for the totality of driver-fuel subassemblies with the input reactivity rate of 5 dollars/sec. The mixed-fuel configuration had less driver fuel than did the all-metal-fuel configuration. To compensate for the feedback due to fuel in the safety, control, and experimental oxide subassemblies, however, the fuel-temperature coefficient of the all-metal configuration, multiplied by the ratio 434/445 (i.e., -3.80×10^{-6} $\Delta k/k\text{-}^{\circ}K$), was used in this first iteration.

2. A special option of MELT-II using input power rather than reactivity as a function of time (see Sect. II.A) was used to run a second problem for the set of safety and control subassemblies. Under this option, a table of the ratio of power at time t to that at time zero is input; a 100-point table was prepared from the results of the first iteration on the driver fuel. The temperature coefficient of the fuel in the safety and control subassemblies was estimated to be -5.21×10^{-7} $\Delta k/k\text{-}^{\circ}K$, as indicated in Sect. II.B.2.

3. This same method was used to run a problem on the experimental oxide subassemblies.

4. A second iteration was then done on the driver-fuel subassemblies, with two modifications of the input. First, instead of the 5-dollar/sec input ramp, a 50-point table of reactivity as a function of time was input. Each point was computed by modifying the input reactivity to account for effects due to expansion and collapse of fuel in the safety, control, and oxide subassemblies, as determined from the problems in 2 and 3 above. Second, the temperature coefficient of the driver fuel was reduced from -3.80×10^{-6} to -3.12×10^{-6} $\Delta k/k\text{-}^{\circ}K$ to account for the smaller amount of driver fuel in the mixed-fuel configuration.

D. Cases Studied

Seven cases were studied for the all-metal-fuel core. The first six were input reactivity ramps of 0.5, 1, 5, 10, 20, and 50 dollars/sec, with the reactor initially at source power (8 W) and 5.5% of the full flow rate. The seventh was for an input ramp of 5 dollars/sec, with the reactor

initially at full power and flow. Eight cases were studied for the hypothetical oxide-fuel core initially at source power and 5.5% flow. Four of these were for input ramps of 1, 5, 10, and 50 dollars/sec, with a fuel-expansion reactivity coefficient equal to that of the all-metal-fuel core; the other four were for the same ramps, but a fuel-expansion coefficient that was one-third that of the all-metal-fuel core. One case was studied of a mixed-fuel configuration initially at source power and 5.5% flow, with an input ramp of 5 dollars/sec.

III. RESULTS

Results obtained for the three types of cores included changes in reactivity with time after a ramp began, sequence of slumping, peak fuel temperature, total power, total reactivity, collapse reactivity, and peak net reactivity.

A. Metal Fuel

Results of the cases studied for the all-metal-fuel reactor initially at 8 W and 5.5% of the full flow rate are summarized in Tables II and III and Figs. 5-7. Table II shows that temperatures characteristic of core disassembly (4419°K) would be attained only for input ramps of 20 dollars/sec or greater. Also, for input ramps of 20 dollars/sec or less, the net output reactivity rates would be actually negative; i.e., the collapse reactivity rates would be negative and large at the point at which the fuel temperature peaks.

TABLE II. MELT-II Results for All-metal-fuel Configuration in EBR-II Initially at Source Power (8 W) and 5.5% of Full Flow Rate

$\dot{k}_{in}$, ¢/sec	Time after Start of Transient, sec	Total Power in Driver Subassemblies, MWt	Total Energy Release in Driver Subassemblies, MWt-sec	Peak Fuel Temperature, °K	Net Reactivity, ¢	Collapse Reactivity, ¢	Collapse Reactivity Rate, ¢/sec	Total Reactivity Rate,[a] ¢/sec	Peak Net Reactivity in Transient, ¢
0.5	2.3557	900	176	3701[b]	91.4	52.0	-5.4	-4.9	100.56
1.0	1.2674	891	175	3676[b]	91.2	42.7	-7.5	-6.5	101.19
5.0	0.3150	783	165	3438[b]	90.26	5.2	-10.6	-5.6	103.51
10.0	0.1750	1005	168	3744[b]	92.07	-4.5	-13.6	-3.6	105.26
20.0	0.10313	1438	187	4420[c]	93.74	-17.4	-20.9	-0.9	107.78
50.0	0.03914	6040	164	4426[c]	98.7	-1.0	-5.4	44.6	112.94

[a]Input rate plus collapse rate.
[b]Peak temperature attained in transient; rapid disassembly does not occur.
[c]Assumed near threshold for rapid disassembly.

TABLE III. Collapse Sequence in All-metal-fuel Core for Different Input Reactivity Rates and Initial Conditions

$\dot{k}_{in}$, ¢/sec	Time to Start of Collapse in Row 1, sec	Time between Start of Collapse in Row n and Start of Collapse in Row 1, msec					
		n = 1	2	3	4	5	6
1[a]	1.1953	0	4.7	15.4	34.1	44.7	71.0
5[a]	0.26493	0	1.3	5.7	14.7	23.8	57.6
20[a]	0.066974	0	0.3	1.8	5.5	10.3	28.0
5[b]	0.24562	0	1.3	5.4	13.3	20.5	41.8

[a]Core initially at 8 W and 5.5% of full flow rate.
[b]Driver fuel initially at 51.2 MWt and full flow rate.

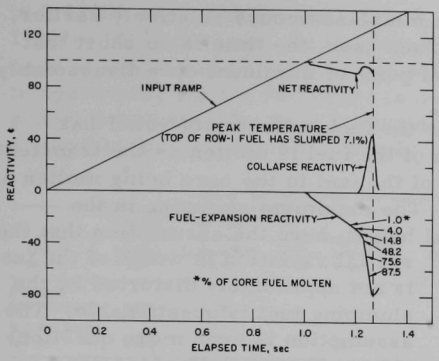

Fig. 5. Change in Reactivity with Time for All-metal-fuel Core Initially at 8-W Power and 5.5% of Full Flow Rate; 1-dollar/sec Input Ramp

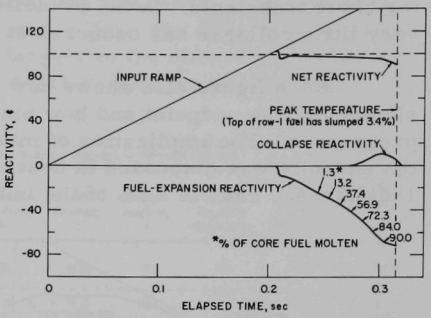

Fig. 6. Change in Reactivity with Time for All-metal-fuel Core Initially at 8-W Power and 5.5% of Full Power Rate; 5-dollar/sec Input Ramp

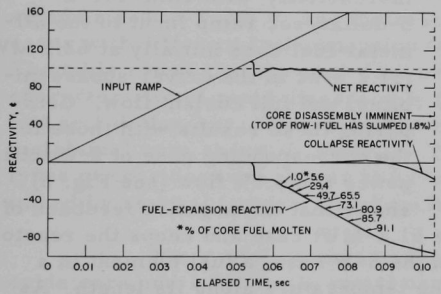

Fig. 7. Change in Reactivity with Time for All-metal-fuel Core Initially at 8-W Power and 5.5% of Full Flow Rate; 20-dollar/sec Input Ramp

The reactivity components for three of the cases are shown in Figs. 5-7. In all three cases, the collapse reactivity would increase to a maximum and then fall off. This change is due to the spatial noncoherence of the collapse (which results from the radially and axially peaked power distribution in the core) and the correspondingly peaked distribution of fuel worth. The fuel near the midplane of the center subassembly begins to collapse first; this collapse causes fuel above it to slump toward the midplane region of the highest worth. Then fuel progressively farther below the midplane begins to slump, and eventually the net movement is away from the midplane. While this collapse pattern is developing in the center subassembly, slumping starts at the midplane of the second row, then the third, fourth, etc. Table III shows the collapse sequence by row for the three cases. Figures 5-7 also show that peak collapse reactivity decreases with increasing input reactivity, i.e., as the time remaining for slumping decreases. In the three cases shown, the collapse reactivity has peaked and is decreasing at the time after the start of the transient given in Table II--hence the negative collapse rates. The collapse reactivity at this time decreases with increasing ramp rates up to and including 20 dollars/sec because the slumping is axially, as well as radially, more nearly coherent;

i.e., net fuel movement away from the midplane occurs relatively earlier, for short transients. In the 50-dollar/sec case, the time is so short that very little collapse has occurred at the point of imminent core disassembly.

Each figure also shows how far the fuel in the top of row 1 has slumped at the endpoint and how much of the fuel is molten as the transient progresses. The implication of most of the fuel in the core being molten at the endpoint was discussed in Sect. I. The maximum slumping in the 1-dollar/sec case is 7.1% of the initial height; here the assumption that the spatial variation in worth of the fuel is not appreciably distorted by the slumping fuel is questionable. The assumption is even more questionable in the 0.5-dollar/sec case, where the corresponding slumping is 8.1%.

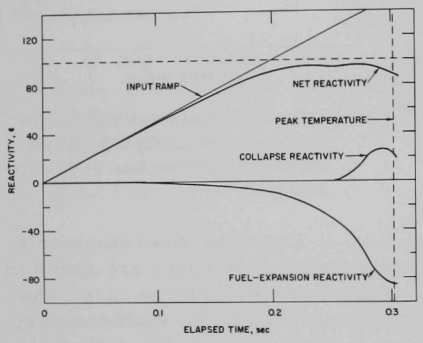

Fig. 8. Change in Reactivity with Time for All-metal-fuel Core Initially at Full Power and Flow; 5-dollar/sec Input Ramp

Figure 8 shows the changes in reactivity with time for a 5-dollar/sec ramp input to the all-metal-fuel core initially at 62.5 MWt (51.2 MWt in the driver subassemblies) and full coolant flow. Comparing these results with those for the corresponding case of 8-W initial power and 5.5% flow (see Fig. 6) shows that the negative feedback of fuel expansion begins earlier with the 51.2-MWt case and keeps the reactor from going super-prompt critical. In the 8-W case, a fuel element in a given row is initially at about the same temperature along its length. As the transient progresses, the temperature at a given radius within the fuel follows the axial shape of the power; i.e., it peaks at the midplane. Fuel slumping thus begins toward the midplane, but soon progresses below it. In the 51.2-MWt case, however, the fuel-surface temperature initially peaks at the core top. As the transient progresses, the peak temperature at the fuel surface moves down toward the midplane, but is still above it at the point of initial fuel collapse. This results in a greater pileup of fuel near the midplane before slumping below it begins, with a consequent greater collapse reactivity. This effect is somewhat enhanced by the shorter times between initial collapse in successive rows, as shown in Table III.

Results of the calculations for the two foregoing cases are compared in Table IV. The peak fuel temperature is considerably higher for the initial-full-power case, although it is below the temperature assumed to be characteristic of disassembly (4419°K). The rise in peak fuel temperature in each case is roughly proportional to the total energy release in the driver subassemblies. The difference between the energy releases for the two cases is 32 MWt-sec. For 8-W initial power, prompt criticality is reached

in 0.20000 sec; at this point, the total energy release in the driver fuel is 1.067×10^{-5} MWt-sec. At this same time, the total energy release in the case of initial full power is 32.15 MWt-sec. Thus, the difference in peak temperatures for the two cases is due largely to the difference in energy generation during the time required to reach prompt criticality with negligible fuel-expansion feedback.

TABLE IV. Effects of Different Initial Conditions on 5-dollar/sec Transient in All-metal-fuel Core

Initial Reactor Conditions	Time after Start of Transient, sec	Total Power in Driver Subassemblies, MWt	Total Energy Release in Driver Subassemblies, MWt-sec	Peak Fuel Temperature,[a] °K	Net Reactivity, ¢	Collapse Reactivity, ¢	Collapse Reactivity Rate,[b] $/sec	Total Reactivity Rate,[b] $/sec	Peak Net Reactivity in Transient, ¢
8 W power; 5.5% of full flow	0.3150	783	165	3438	90.26	5.2	-10.6	-5.6	103.51
51.2 MWt power; full flow	0.3022	1173	197	4139	88.46	22.5	-9.8	-4.8	95.58

[a]Peak temperature attained in transient; rapid disassembly does not occur.
[b]Input rate plus collapse rate.

B. Oxide Fuel

Results of the calculations for the hypothetical oxide-fuel core are summarized in Table V, and the reactivity features of the two 5-dollar/sec cases with different fuel-expansion feedbacks are shown in Figs. 9 and 10. The table shows that the peak fuel temperature reaches the point assumed characteristic of rapid disassembly (3950°K), even for an input ramp as low as 1 dollar/sec. This result is in contrast to the results for the all-metal-fuel core shown in Table II. The difference in behavior of the two types of core does not appear to have a simple explanation, but is determined by several factors, which include the following:

1. The radial peak-to-average power distribution is 1.258 in the oxide core and 1.316 in the metal core.

2. The oxide fuel retains more of the energy generated in it than does the metal fuel, because the oxide has a gas bond and the metal a sodium bond.

TABLE V. MELT-II Results for Hypothetical Oxide-fuel Configuration in EBR-II Initially at Source Power (8 W) and 5.5% of Full Flow Rate

$\dot{k}_{in}$, $/sec	Time after Start of Transient, sec	Total Power in Driver Subassemblies, MWt	Total Energy Release in Driver Subassemblies, MWt-sec	Peak Fuel Temperature,[a] °K	Net Reactivity, ¢	Collapse Reactivity, ¢	Collapse Reactivity, Rate, $/sec	Total Reactivity Rate,[b] $/sec	Peak Net Reactivity in Transient, ¢
1.0[c]	1.8356	12,250	361	3949	99.03	77.7	24.7	25.7	102.32
5.0[c]	0.5056	5,358	359	3947	97.4	8.8	6.9	11.9	106.63
10.0[c]	0.2592	6,668	359	3947	97.5	5.0	3.4	13.4	109.89
50.0[c]	0.05353	22,110	359	3957	98.5	0.5	0.1	50.1	124.25
1.0[d]	1.4226	8,459	360	3957	99.2	11.1	8.3	9.3	102.49
5.0[d]	0.3033	13,190	358	3942	98.7	2.9	1.7	6.7	106.94
10.0[d]	0.1543	19,840	358	3943	99.0	0.9	0.3	10.3	110.30
50.0[d]	0.03247	149,800	360	3950	106.22	0.6	1.0	51.0	125.10

[a]Assumed near threshold for rapid disassembly.
[b]Input rate plus collapse rate.
[c]Fuel-expansion reactivity effect = -3.9×10^{-6} $\Delta k/k$-°K.
[d]Fuel-expansion reactivity effect = -1.3×10^{-6} $\Delta k/k$-°K.

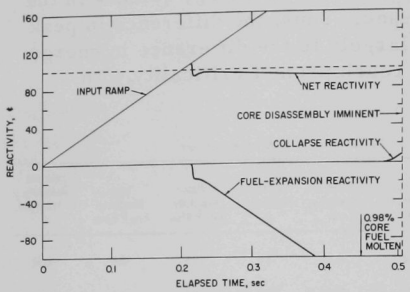

Fig. 9. Change in Reactivity with Time for Hypothetical Oxide-fuel Core Initially at 8-W Power and 5.5% of Full Flow Rate; $\Delta k/k\text{-}^{o}K = -3.9 \times 10^{-6}$; 5-dollar/sec Input Ramp

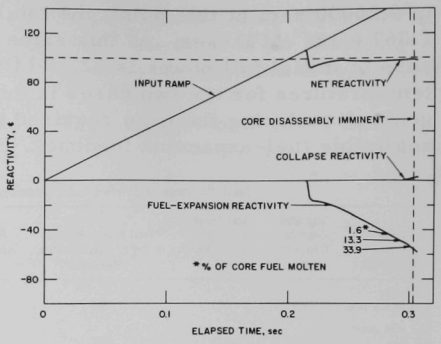

Fig. 10. Change in Reactivity with Time for Hypothetical Oxide-fuel Core Initially at 8-W Power and 5.5% of Full Flow Rate; $\Delta k/k\text{-}^{o}K = -1.3 \times 10^{-6}$; 5-dollar/sec Input Ramp

3. The ratio of total heat content of fuel in the oxide core to that in the metal core increases markedly with temperature, being 0.905 at 644°K, 1.68 between 644 and 3040°K, and 2.35 between 644 and 3950°K.

4. The assumed disassembly temperature is 3950°K for the oxide fuel and 4419°K for the metal fuel.

5. The prompt-neutron generation time is 2.20×10^{-7} sec for the oxide core and 0.793×10^{-7} sec for the metal core.

6. The two cores are in different states of collapse at the times indicated in Tables II and V.

These factors interact in a complex manner to produce a strongly nonlinear feedback reactivity that determines the power as a function of time. The integrated power, in turn, affects not only the ultimate peak fuel temperature but also the feedback reactivity.

The flatter radial power distribution in the oxide core causes the peak fuel temperature in this core to be nearer the average-core-fuel temperature than in the metal core. Since disassembly is assumed imminent when the peak temperature reaches a specified value, the effect of radial power distribution alone would imply earlier trouble in the metal core. But the effects of energy retention in the fuel and disassembly temperature also must be considered. The metal fuel retains less of the energy generated in it, because its sodium bond conducts significant heat to the bond, cladding, and coolant. This conductance is the reason for the large difference in fuel-expansion reactivity at the end points between:

1. The all-metal-fuel core at source initial conditions, with a 5-dollar/sec input ramp (see Fig. 6), and

2. The all-oxide fuel core at source initial conditions, with the same fuel-expansion coefficient and input ramp (see Fig. 9). Row-1 mid-plane temperatures (°K), of the two cores would be:

	Metal	Oxide
Fuel center	3438	3947
Outer radial node	2372	3251
Cladding	1845	1125
Coolant	1616	1027
Core average (fuel)	1977	3079

The energy-retention effect thus tends to work opposite the radial-peaking effect. This is also true of the greatly different disassembly temperatures of the two fuels.

For all cases studied, about twice as much total energy is generated in the oxide core as in the metal core. This difference, seen by comparing the fourth columns of Tables II and V, is consistent with the heat content of the oxide fuel, being about twice that of the metal fuel for comparable final peak fuel temperatures; comparing heat contents of metal and oxide is complicated by the better heat transfer of the metal-fuel element. For a given fuel-feedback coefficient, the longer time scale for a transient in the oxide core results directly from the greater heat content of this core, but again the relationship is complicated by the effects mentioned in Sect. II.B.2. Effects of a smaller fuel-expansion feedback coefficient of the oxide fuel are shown in Table V and Fig. 10. Although the total energy generated is nearly independent of the fuel-expansion feedback coefficient, the transient is shorter for the cores with the smaller coefficient.

Some insight into the effect of generation time for prompt neutrons is obtained by considering the change of net reactivity and power with time of the metal and oxide cores that start at source power, with the same fuel-expansion feedback coefficient and 5-dollar/sec input ramp (see Figs. 11 and 12). The metal core reaches prompt criticality at 1.95×10^{-3} MWt, and the oxide core at 0.98×10^{-3} MWt; the difference results largely from the differences in neutron-generation time. Because of its relatively long generation time, the oxide core has reached a power of only 0.057 MWt at the point where the input reactivity is 103.5 cents; i.e., insignificant fuel heating and resulting feedback have occurred. In the metal core, however, at 0.2073 sec and 103.5 cents of input reactivity, the power has increased to 763 MWt and the energy generated is 0.248 MWt-sec; here fuel expansion begins to reduce the net reactivity. In the oxide core, the net reactivity peaks at 0.2139 sec and 106.6 cents, at a power of 762 MWt and energy generated of 0.448 MWt-sec.

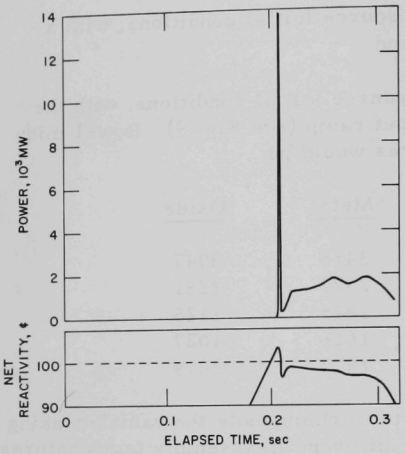

Fig. 11. Change in Net Reactivity and Power with Time for All-metal-fuel Core Initially at 8-W Power and 5.5% of Full Flow Rate; 5-dollar/sec Input Ramp

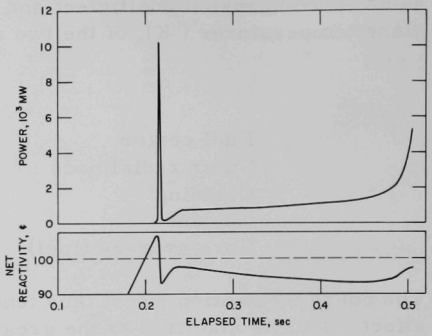

Fig. 12. Change in Net Reactivity and Power with Time for Hypothetical Oxide-fuel Core Initially at 8-W Power and 5.5% of Full Flow Rate; $\Delta k/k\text{-}^{o}K = -3.9 \times 10^{-6}$; 5-dollar/sec Input Ramp

At 0.2085 sec, the net reactivity of the metal core has decreased to 100 cents, with an increase in power to 13,870 MWt. The net reactivity of the oxide core has decreased to 100 cents at 0.2160 sec, with a power increase to 10,190 MWt. In this interval, the power in the metal core has increased faster, primarily because of its shorter generation time. In both cases, as the net reactivity falls below 100 cents, the power begins to decrease. The net reactivity of the metal core decreases to a minimum of 96.5 cents at 0.2097 sec; here its power is 1244 MWt, and the total energy generated is 15.69 MWt-sec. The oxide core has greater fuel-expansion feedback because of the greater total energy generation in its fuel. Its minimum net reactivity is thus less--93.15 cents at 0.2182 sec. Here the power is reduced to 709 MWt, and the energy generated is 21.03 MWt-sec. The greater net reactivity of the oxide core also contributes to its ultimate failure. Figures 11 and 12 show the relationships between net reactivity and power over the course of the two transients. Figure 13 shows the corresponding history for the oxide with smaller fuel-expansion feedback.

Near the end of the transient, the state of core collapse has an important effect on the variation with time of net reactivity, and hence power, for collapse rates less than about 20 dollars/sec. For the metal core, the relatively low melting point of the metal fuel leads to early collapse. At the end of the transient, the collapse rate and the fuel-expansion reactivity rate are negative, as is shown for the 5-dollar/sec case in Fig. 6. Together these effects override the input ramp and sharply reduce the net

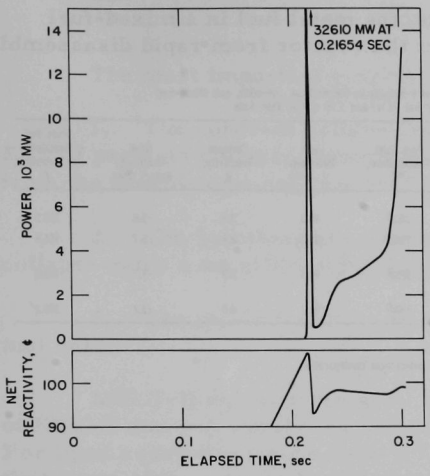

Fig. 13. Change in Net Reactivity and Power with Time for Hypothetical Oxide-fuel Core Initially at 8-W Power and 5.5% of Full Flow Rate; $\Delta k/k\text{-}^{o}K = -1.3 \times 10^{-6}$; 5-dollar/sec Input Ramp

reactivity, leading to a power reduction, as shown in Fig. 11. For the oxide core with the same fuel-expansion coefficient and same input ramp, fuel collapse begins much later, owing to the high melting point of the oxide (see Fig. 9). Up to the point where the collapse reactivity begins, the fuel-expansion reactivity holds the net reactivity nearly flat. The strongly positive collapse reactivity rate, however, causes the net reactivity rate, and hence power, to increase rapidly near the end of the transient (see Fig. 12). This increase appears to be important in the tendency of the oxide core to approach conditions of rapid disassembly for even the lowest input ramps studied.

Figure 14 shows the reactivity components for the most severe case studied, a 50-dollar/sec input ramp to the hypothetical oxide-fuel core, initially at source conditions, and a fuel-feedback coefficient equal to one-third that of the metal-fuel reactor. This case is the only one of all those studied in this work where the rate of change of total reactivity is positive and the system is super-prompt critical at the point of imminent disassembly. For the short time scale of this transient, fuel collapse is not important.

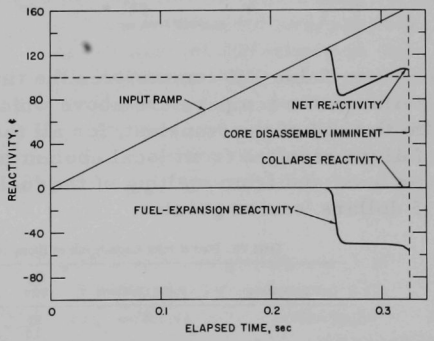

Fig. 14. Change in Reactivity with Time for Hypothetical Oxide-fuel Core Initially at 8-W Power and 5.5% of Full Flow Rate; $\Delta k/k\text{-}^{o}K = -1.3 \times 10^{-6}$; 50-dollar/sec Input Ramp

The effective delayed-neutron fraction and prompt-neutron generation time for the mixed-fuel configuration are both close to the corresponding values for the all-metal-fuel core, as shown in Table I. Thus, because the mixed-fuel core contained a predominance of metal driver fuel, the behavior of this core in a given transient would be expected to be similar to that of the all-metal-fuel core. That this is true is shown in Table VI. The reactivity effects for the mixed-fuel case (see Fig. 15) show that the safety and control rods contribute little to the collapse reactivity and that the oxide fuel does not

collapse at all in the time shown. Thus, the metal fuel in a mixed-fuel configuration acts as a fuse to protect the reactor from rapid disassembly.

TABLE VI. MELT-II Results for 5-dollar/sec Ramp Insertion of Reactivity in Wet-critical, All-oxide, and Mixed-fuel Configurations of EBR-II Initially at Source Power (8 W) and 5.5% of Full Flow Rate

Core Configuration	Time after Start of Transient, sec	Total Power in Driver Subassemblies, MWt	Total Energy Release in Driver Subassemblies, MWt-sec	Peak Fuel Temperature, °K	Net Reactivity, ¢	Collapse Reactivity, ¢	Total Reactivity, Rate,[a] ¢/sec	Peak Net Reactivity in Transient, ¢
All metal (wet-critical)	0.3150	783	165	3438[b]	90.3	5.2	-5.6	103.5
All-oxide[c]	0.3033	1.32×10^4	358	3942[d]	98.7	2.9	6.7	106.9
Mixed fuel, first iteration	0.3187	598	124	3228[b]	90.5	2.9	-3.7	103.8
Mixed fuel, second iteration	0.3235	619	127	3304[b]	90.7	4.0	-3.7	103.2

[a]Input rate plus collapse rate.
[b]Peak temperature attained in transient; rapid disassembly does not occur.
[c]Oxide-fuel temperature coefficient of reactivity taken as one-third that of metal fuel in wet-critical configuration.
[d]Assumed near threshold for rapid disassembly.

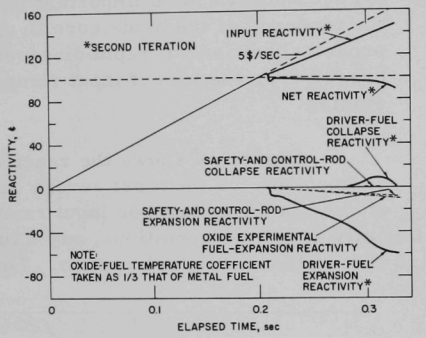

Fig. 15
Change in Reactivity with Time for Mixed-fuel Configuration Initially at 8-W Power and 5.5% of Full Flow Rate; 5-dollar/sec Input Ramp

Table VII summarizes the time to initial fuel collapse (i.e., cladding failure), the temperature above which initial collapse results, and the time to the end of the transient, for all the cases studied. In all cases, cladding failure resulted from local coolant boiling for input ramps of 1 dollar/sec or less, and from melting of the fuel near its surface for input ramps of 5 dollars/sec or greater.

TABLE VII. Effect of Input Reactivity Rate on Elapsed Times to Initial Fuel Collapse and to Incipient Disassembly

Core Configuration	Initial Conditions	k_{in}, ¢/sec	Time to Initial Collapse, sec	Temperature Causing Initial Collapse, °K	Time to End of Transient, sec
All metal fuel	8 W; 5.5% flow	0.5	2.278	$T_c \geq 1153$[a]	2.356
		1.0	1.195	$T_c \geq 1153$	1.267
		5.0	0.2649	$T_f \geq 1293$[b]	0.3150
		10.0	0.1343	$T_f \geq 1293$	0.1750
		20.0	0.06697	$T_f \geq 1293$	0.1031
		50.0	0.02706	$T_f \geq 1293$	0.03914
All metal fuel	Full power and flow	5.0	0.2456	$T_f \geq 1293$	0.3022
Hypothetical oxide fuel	8 W; 5.5% flow; $(\Delta k/k\text{-}°K)_{fuel}$ = -3.9×10^{-6}	1.0	1.766	$T_c \geq 1153$	1.836
		5.0	0.4732	$T_f \geq 3040$	0.5056
		10.0	0.2347	$T_f \geq 3040$	0.2592
		50.0	0.04591	$T_f \geq 3040$	0.05353
	8 W; 5.5% flow; $(\Delta k/k\text{-}°K)_{fuel}$ = -1.3×10^{-6}	1.0	1.389	$T_c \geq 1153$	1.423
		5.0	0.2865	$T_f \geq 3040$	0.3033
		10.0	0.1432	$T_f \geq 3040$	0.1543
		50.0	0.02606	$T_f \geq 3040$	0.03247
Mixed fuel	8 W; 5.5% flow	5.0	0.2456	$T_f \geq 1293$	0.3022

[a]T_c = peak coolant temperature.
[b]T_f = peak temperature in outermost radial fuel node.

IV. CONCLUSIONS

The most important conclusions from this work are:

1. The coherent collapse model used in early safety analyses of EBR-II predicts collapse ramp rates much greater than those obtained from the noncoherent collapse model in the MELT-II code.

2. The hypothetical oxide-fuel configuration would have positive collapse rates even at low input ramps.

3. The mixed fuel core would behave much like the all-metal-fuel core.

MELT-II calculations were made on an all-metal-fuel configuration of EBR-II that was similar to that of the core studied in the earlier analyses. For input reactivity ramps from 0.5 to 50.0 dollars/sec, the collapse reactivity rate always would be negative where the fuel temperature peaked or approached the value at which disassembly was assumed imminent. Further, in all these cases, the net reactivity would be less than 1 dollar at this point. For input ramps of 10 dollars/sec or less, the maximum fuel temperature would peak below the assumed disassembly temperature; here a benign failure rather than rapid disassembly of the core would be expected. With an input ramp of 20 dollars/sec or greater, an increasingly severe disassembly condition would be expected.

The reactor with the hypothetical oxide fuel, on the other hand, would have positive collapse rates for input ramps from 1 to 50 dollars/sec, for two different fuel-feedback coefficients. This important difference in collapse characteristics is closely related to the higher melting point and lower boiling point of the oxide fuel. In all cases studied here, the peak fuel temperature would reach the point assumed characteristic of rapid disassembly although the net reactivity would be greater than 1 dollar for only a 50-dollar/sec input ramp with a fuel-expansion coefficient one-third that of the all-metal core.

A core typical of current EBR-II irradiation configurations, i.e., metal driver fuel with some oxide fuel, would behave much like the all-metal-fuel core with a 5-dollar/sec input ramp. The metal fuel would melt, collapse away from the core midplane, and reach its peak temperature before the oxide fuel would begin to melt. That is, the metal fuel would protect the core from rapid disassembly. Thus, for maximum protection of EBR-II, some metal fuel should be in the core, near its center.

Desirable future work in this area would include further checking out of the subroutine for sodium voiding and including the spatial dependence of the fuel-expansion reactivity coefficient.

ACKNOWLEDGMENTS

Acknowledgment is made of help given by A. E. Waltar of WADCO and L. B. Miller of ANL in making the MELT-II Code operational on the Argonne IBM 360/75 computer.

REFERENCES

1. L. J. Koch *et al.*, *Hazard Summary Report: Experimental Breeder Reactor II (EBR-II)*, ANL-7519 (May 1957).

2. L. J. Koch, W. B. Loewenstein, and H. O. Monson, *Addendum to Hazard Summary Report: Experimental Breeder Reactor-II (EBR-II)*, ANL-5719 (Addendum) (June 1962).

3. V. Z. Jankus, "A Modified Equation of State for Hydrodynamic Calculations in AX1 Numerical Program," *Proceedings of the Conference on Safety, Fuels, and Core Design in Large Fast Power Reactors, October 11-14, 1965*, ANL-7120, pp. 686-691.

4. A. E. Waltar, A. Padilla, Jr., and R. J. Shields, *MELT-II, A Two Dimensional Neutronics-Heat Transfer Computer Program for Fast Reactor Safety Analysis*, WHAN-FR-3, WADCO (to be published).

5. G. H. Golden and B. R. Sehgal, *Thermal-Hydraulic and Doppler Characteristics of Some Oxide Cores for EBR-II*, Trans. Am. Nucl. Soc. *12*(2), 916 (Nov 1969).

6. W. T. Sha and T. H. Hughes, *Coupled Neutronic-Hydrodynamic Fast Reactor Disassembly Analysis*, Trans. Am. Nucl. Soc. *13*(1), 365 (June-July 1970).

7. F. S. Kirn and W. B. Loewenstein, *EBR-II Wet Critical Experiments*, ANL-6864, p. 27 (Oct 1964).

8. J. L. Gillette, G. H. Golden, and B. R. Sehgal, *Neutronic and Thermal-Hydraulic Analyses of Mixed Cores for EBR-II* (to be published).

9. D. A. Meneley, L. C. Kvitek, and D. M. O'Shea, *MACH 1, A One-dimensional Diffusion-theory Package*, ANL-7223 (June 1966).

10. *Reactor Physics Constants*, ANL-5800 (Second Edition) p. 602 (July 1963).

11. *Idaho Division Summary Report: July, August, September 1960*, p. 65, ANL-6301.

12. C. M. Walter and C. E. Dickerman, *TREAT Study of the Penetration of Molten Uranium and U/5 wt % Fs Alloy through Type 304 Stainless Steel*, Nucl. Sci. & Eng. *18*(4), p. 518 (Apr 1964).

13. G. H. Golden and J. V. Tokar, *Thermophysical Properties of Sodium*, ANL-7323 (Aug 1967).

14. H. Savage and R. D. Seibel, *Heat Capacity Studies of Uranium and Uranium-Fissium Alloys*, ANL-6702 (Sept 1963).

15. R. J. Ackermann and E. G. Rauh, *The Vapor Pressure of Liquid Uranium; Effects of Dissolved Tantalum, Phosphorus, Sulfur, Carbon, and Oxygen*, J. Phys. Chem. *73*, 769-778 (Apr 1969).

16. S. T. Zegler and M. V. Nevitt, *Structures and Properties of Uranium-Fissium Alloys*, ANL-6116 (July 1961).

17. A. Waltar, WADCO, private communication.